SUPPORTING INFORMATION

Probe Confined Dynamic Mapping for GPCR Allosteric Site Prediction

Antonella Ciancetta[1#§], Amandeep Kaur Gill[2‡], Tianyi Ding[1], Dmitry S. Karlov[1], George Chalhoub[2], Peter J. McCormick[2] and Irina G. Tikhonova[1]

[1]School of Pharmacy, Medical Biology Centre, Queen's University Belfast, Belfast, Northern Ireland, BT9 7BL, UK

[2]Centre for Endocrinology, William Harvey Research Institute, Bart's and the London School of Medicine and Dentistry, Queen Mary, University of London, London, EC1M 6BQ, UK

[#]Led computational chemistry effort.

[‡]Led molecular pharmacology effort.

[*] Correspondence, Email: i.tikhonova@qub.ac.uk and p.mccormick@qmul.ac.uk

[§] Present Address: Department of Chemical, Pharmaceutical and Agricultural Sciences, University of Ferrara, 44121, Ferrara, Italy

Table S1. The strongest ligand-residue interaction energy (IE) from the triplicate conventional MD simulations trajectories of the X-ray receptor-ligand complexes. Residues selected for allosteric interaction spots are in bold.

Top residues selected from the lowest ligand-residue interaction energy, (kcal/mol)					
[a]M$_2$-LY211960		[b]β$_2$-Cmp-15		[c]P$_2$Y$_1$-BPTU	
E175	**-18**	**D331**	**-30**	**L102**	**-9.9**
Y177	**-13.1**	**S329**	**-12.7**	**T103**	**-5.9**
W422	**-11.4**	**N69**	**-11.3**	**M123**	**-4.9**
N410	-8.7	**R63**	**-9.7**	P105	-3.4
E172	**-7.4**	**L64**	**-6.7**	F119	-2.5
Y80	**-7**	**F332**	**-5.6**	Q127	-1.8
T170	-4.7	K270	-4.8	L126	-1.7
Y426	-3.7	T68	-4.6	F66	-1.4
Tyr83	-3.1	**I72**	**-3.1**	V101	-1.4
N419	**-3**	T274	-2.9	F62	-1.3
F181	-2	A271	-2.4	A106	-1.3
S182	-1.5	**Y326**	**-1.8**	L99	-1
T84	-1.3	A335	-1.8	C124	-0.8
T423	-1.3	P330	-1.7	W117	-0.7
V407	-0.3	**V54**	**-1.6**	I130	-0.5
Y403	-0.2	F61	-1.5		
		I58	**-1.3**		
		R328	-1.3		
		T66	-1.2		
		I334	-1.2		
		I325	-1		
		T73	-0.8		
		L275	**-0.6**		

[a] For the M$_2$ receptor ternary complex with LY211960, we identified the residue establishing the strongest and most persistent electrostatic interactions - E175[ECL2]. This residue initially lied far away from the allosteric site, however, the PAM piperazine ring underwent conformational changes by adopting alternative orientations during the MD simulations. As for the van der Waals contribution to the total IE, the residues most contributing were Y177[ECL2] and W422[7.35].

[b]The ligand consistently shifted toward helices 6-7 interface by ~1.5 Å in all three trajectories. D331[8.49], S329[8.47] and N69[2.40] are the residues mostly contributing via electrostatic interactions to the ligand binding and L64[ICL1] is the residue establishing the strongest and most persistent van der Waals interaction.

[c] Trajectory visual inspection identified that the ligand *p*-trifluoromethyl phenyl ring and, to a lesser extent, the pyridine ring slightly moved away from the transmembrane bundle towards the membrane in all the trajectories. These fluctuations are reflected in the IE analysis, as the residue establishing the strongest and most persistent electrostatic interactions with the ligand is L102[2.55], whereas the strongest and most persistent van der Waals interactions engaged L102[2.55], T103[2.56], P105[2.58], and M123[3.24] sidechains surrounding the ligand t-butyl phenyl and pyridine rings.

Table S2. P2O and PHX probe occupancy at the P₂Y₁ receptor from probe confined dynamic mapping of various helix-lipid interfaces (calculated over five independent trajectories). The amino acid residues forming a binding cavity at the lipid interface and used to define interaction spots are also reported in the table.

Receptor Area at the lipid interface	Binding cavity detected by MDpocket	P2O occupancy, %	PHX occupancy, %
1. Interface of helices 2, 3 and 4 (L95$^{2.48}$, A96$^{2.49}$, I130$^{3.31}$, V133$^{3.34}$, N134$^{3.35}$, W176$^{4.50}$, and V180$^{4.54}$)	Yes	18±18	9±9
2. Interface of helices 3, 4 and 5	No	0	0
3. Interface of helices 6 and 7 (T267$^{6.42}$, V268$^{6.43}$, V271$^{6.46}$, S272$^{6.47}$, L315$^{7.44}$, N316$^{7.45}$, and V319$^{7.48}$)	Yes	25±30	10±17
4. Interface of helices 7 and 1 (F49$^{1.30}$, L54$^{1.35}$, V57$^{1.38}$, V308$^{7.37}$, G311$^{7.40}$, L312$^{7.41}$, and L315$^{7.44}$)	Yes	0	0

Table S3. Pharmacological parameter analysis of Forskolin-Induced cAMP accumulation assays of D_2 receptor wild type and mutants in the absence and presence of UCB compound. Data values correspond to **Figure 4** in the absence and presence of the allosteric modulator. In the absence of the PAM, ΔpEC_{50} is calculated relative to the pEC_{50} of the D_2 WT with dopamine only. In the presence of the PAM, ΔpEC_{50} is calculated relative to the calculated pEC_{50} of the respective construct in the absence of the PAM. Each data value represents the mean ± SEM from three independent experiments, each condition being in triplicate.

	Dopamine			Dopamine + PAM (10 µM)			
	pEC_{50}	ΔpEC_{50}	E_{max} (%)	pEC_{50}	ΔpEC_{50}	E_{max} (%)	ΔE_{max} (%)
D2 WT	9.25 ± 0.12	0.00	11.22 ± 1.87	10.43 ± 0.24	-1.18	32.60 ± 7.23	21.40
V91A	9.06 ± 0.95	-0.19	54.90 ± 7.74	/	/	89.17 ± 12.9	34.27
L94A	8.71 ± 0.54	-0.54	41.97 ± 6.63	/	/	99.14 ± 8.59	57.17
L94W	9.72 ± 0.31	0.47	12.56 ± 2.72	10.02 ± 0.66	0.30	35.64 ± 6.21	23.08
E95A	9.12 ± 0.97	-0.13	27.44 ± 3.73	11.91 ± 0.97	2.79	63.10 ± 4.80	35.66
W100A	8.11 ± 0.75	-1.14	49.11 ± 13.8	-	-	-	-
I184A	8.29 ± 0.11	-0.96	28.67 ± 2.58	-	-	-	-
W413A	8.83 ± 0.59	-0.42	24.39 ± 3.99	11.87 ± 0.87	3.04	30.54 ± 1.33	6.15

Table S4 Primer Sequences for Site-Directed Mutagenesis of the D$_2$ Mutants. Both the forward (*FW*) and reverse (*RV*) primer sequences used for site-directed mutagenesis of the D$_2$ mutants, using the D$_{2L}$ plasmid as the template, are denoted in the 5' to 3' direction. All primers were designed using Benchling. Mutated residues are indicated in red.

Mutant	Template		Primer Sequence (5'→ 3')
pcDNA3.1 - D$_{2L}$ L94W	pcDNA3.1 - D$_2$	*FW*	CTACTGGGAGGTGGTAGGTGAGTGGAAATTC
		RV	CACCTCCCAGTAGACAACCCAGGGCAT
pcDNA3.1 - D$_{2L}$ E95A	pcDNA3.1 - D$_2$	*FW*	CCTGGCGGTGGTAGGTGAGTGG
		RV	ACCGCCAGGTAGACAACCCAGG
pcDNA3.1 - D$_{2L}$ W100A	pcDNA3.1 - D$_2$	*FW*	GTGAGGCGAAATTCAGCAGGATTCACT
		RV	ATTTCGCCTCACCTACCACCTCCAGG
pcDNA3.1 - D$_{2L}$ L94A	pcDNA3.1 - D$_2$	*FW*	CTACGCGGAGGTGGTAGGTGAGTGGAAATTC
		RV	CCTCCGCGTAGACAACCCAGGGC
pcDNA3.1 - D$_{2L}$ V91A	pcDNA3.1 - D$_2$	*FW*	CTGGGCTGTCTACCTGGAGGTGG
		RV	GACAGCCCAGGGCATGACCAGT
pcDNA3.1 - D$_{2L}$ I184A	pcDNA3.1 - D$_2$	*FW*	GCATCGCTGCCAACCCGGCCTT
		RV	GCAGCGATGCACTCGTTCTGGTCTG
pcDNA3.1 - D$_{2L}$ W413A	pcDNA3.1 - D$_2$	*FW*	CACGGCGCTGGGCTATGTCAACAGCG
		RV	CAGCGCCGTGAAGGCGCTGTACAG

Figure S1. Search for privileged fragments from known allosteric modulators. Maximum common substructure search for the muscarinic PAMs led to Structure 1. Fragmentation of structures of the known NAM for the β_2 and P_2Y_1 receptors. The ligand structure was fragmented by functional groups for both the β_2 and P_2Y_1 receptors.
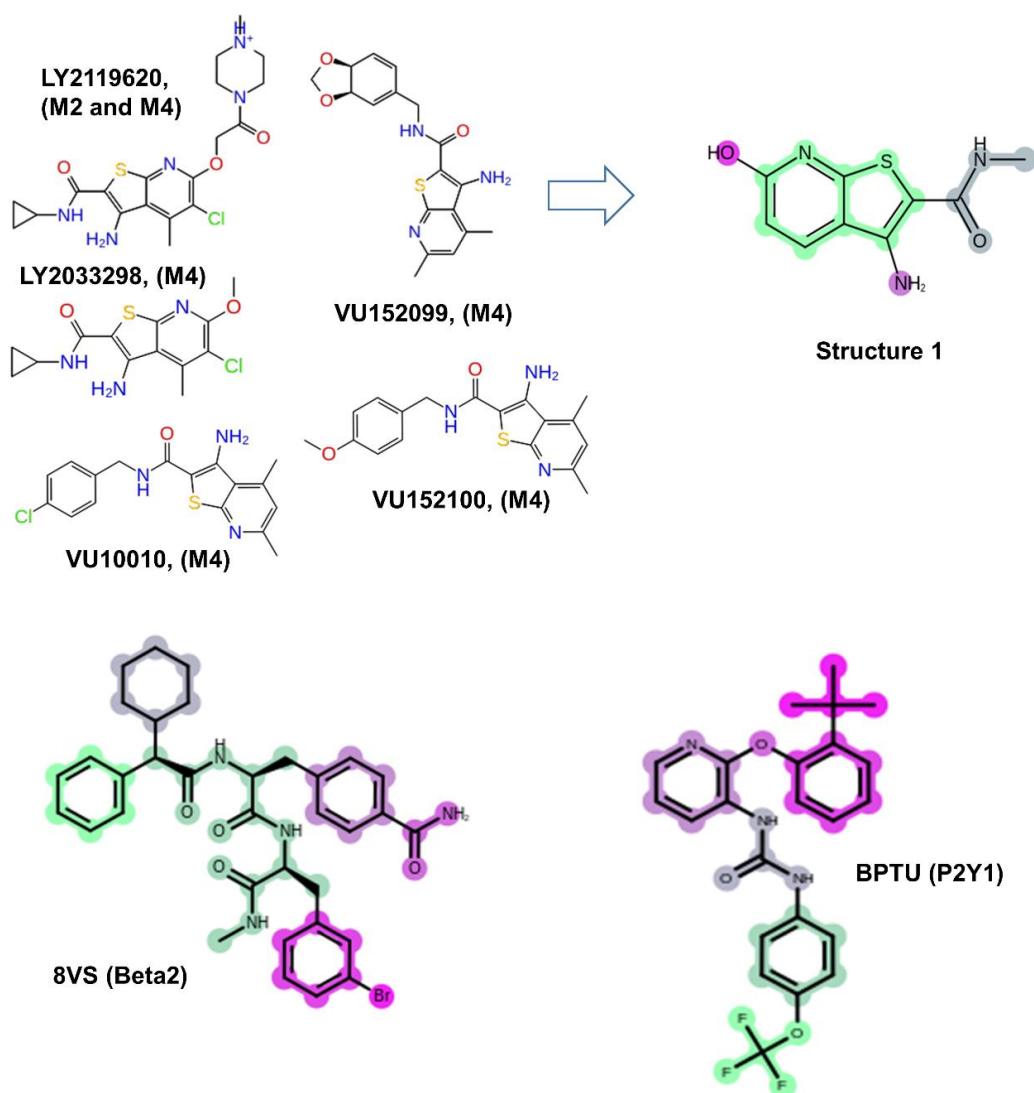
Figure S2. Probe positions and interactions in the allosteric site of the M₂ receptor. The probe molecules and the orthosteric ligand are shown with green and orange carbon atoms, respectively. Only the residues that are used for probe interaction spots are shown in stick-like representation. Hydrogen bonds and π-π interactions are shown in black and cyan dashed lines, respectivly. A MD snapshot with the probe occupying the allosteric site was selected to generate the images.
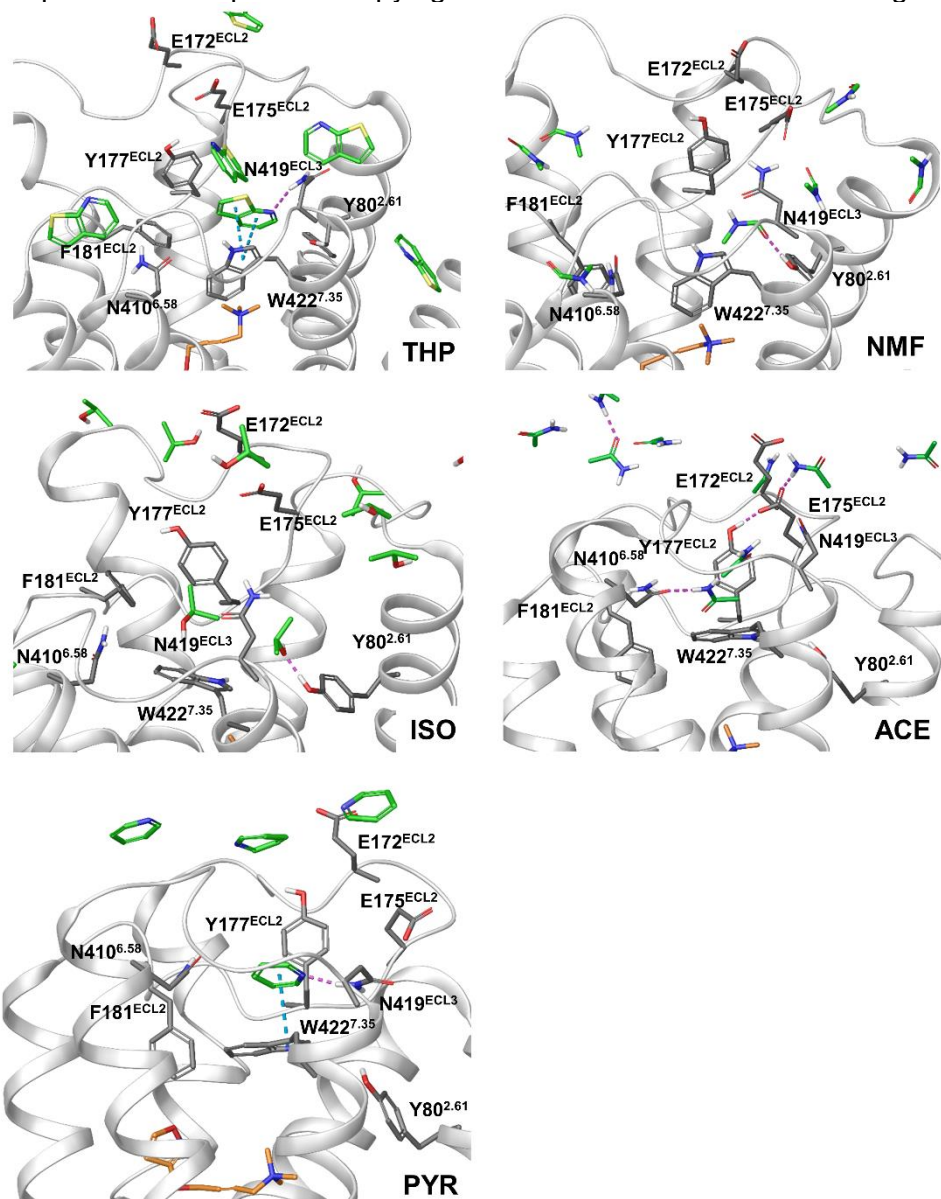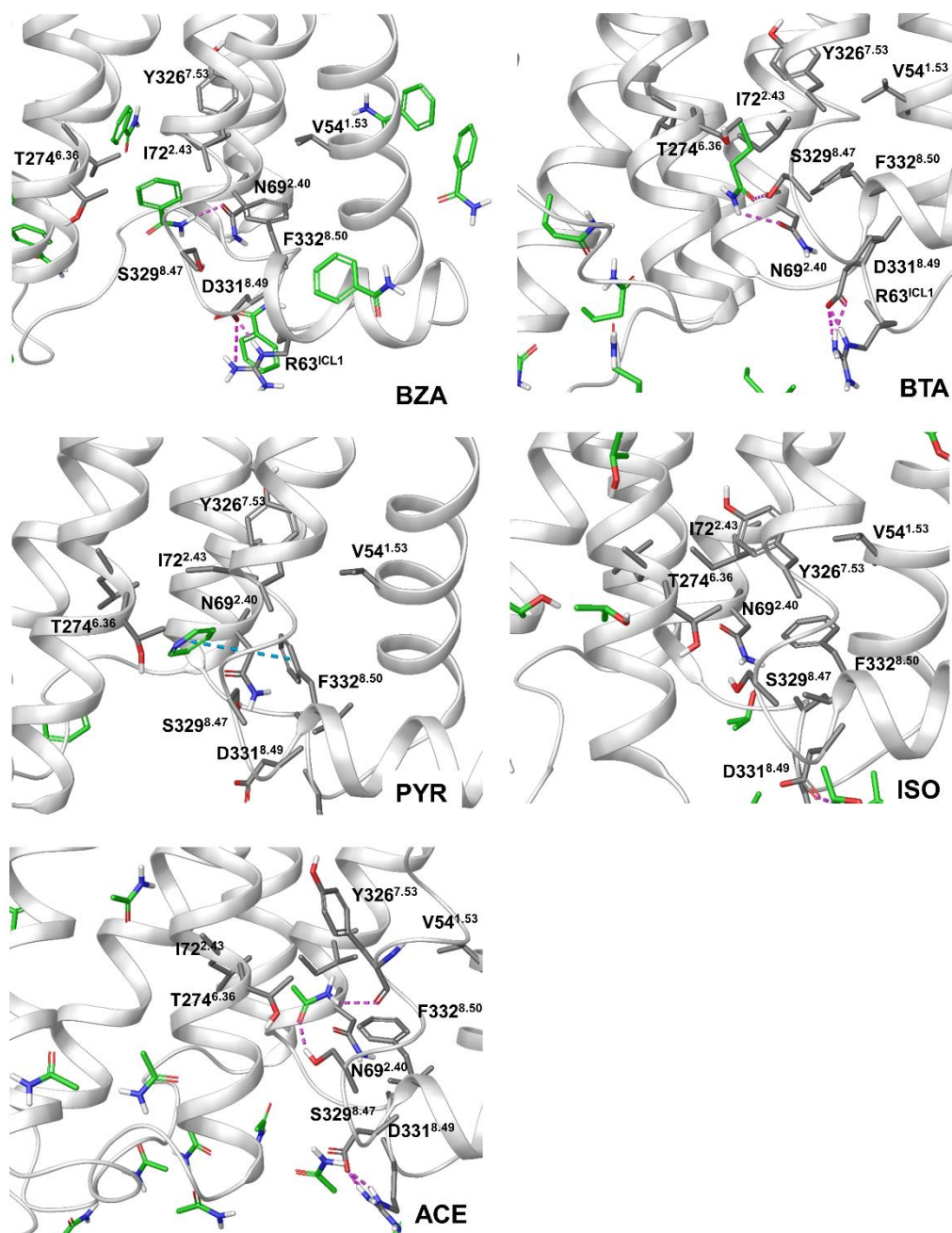
Figure S3. Probe positions and interactions in the allosteric site of the β₂ receptor. Probe molecules are shown with green carbon atoms. Only the residues used for probe interaction spots are shown in stick-like representation. Hydrogen bonds and π-π interactions are shown in black and cyan dashed lines, respectivly. A MD snapshot with probe occupying the allosteric site was selected to generate the images.

Figure S4. Probe positions and interactions in the allosteric site of the P$_2$Y$_1$ receptor. Probe molecules are shown with green carbon atoms. Only the residues that are used for probe interaction spots are shown in stick-like representation, respectivly. Hydrogen bonds and π-π interactions are shown in black and cyan dashed lines, respectivly. A MD snapshot with the probes occupying the allosteric site was selected to generate the images.
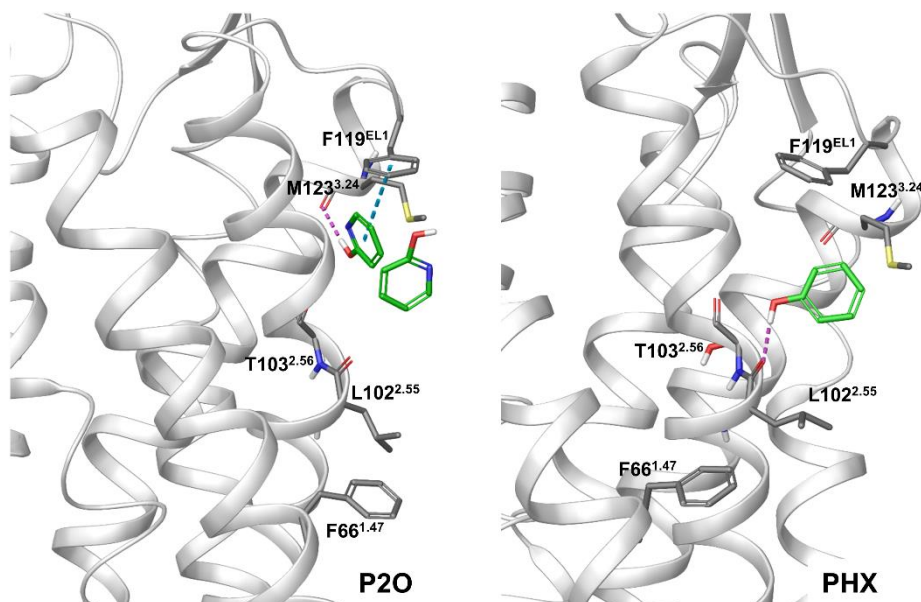
Figure S5. The cylinder-shaped harmonic wall potential with addition of two collective variables (CV1 and CV2) to confine the movement of the probes at the lipid interface of helices 2-4 (A), helices 3-5 (B) and helices 1-6-7 (C) in the P2Y1 production simulations. The collective variables that define a cylinder were selected with lower and upper boundaries (10 and 35 Å). The wall potential in **C** shows the sampling of cavities at the interface of 6 and 7 and at the interface of 1 and 7 (Table S2). Only transmembrane helices are shown in rainbow cartoon.
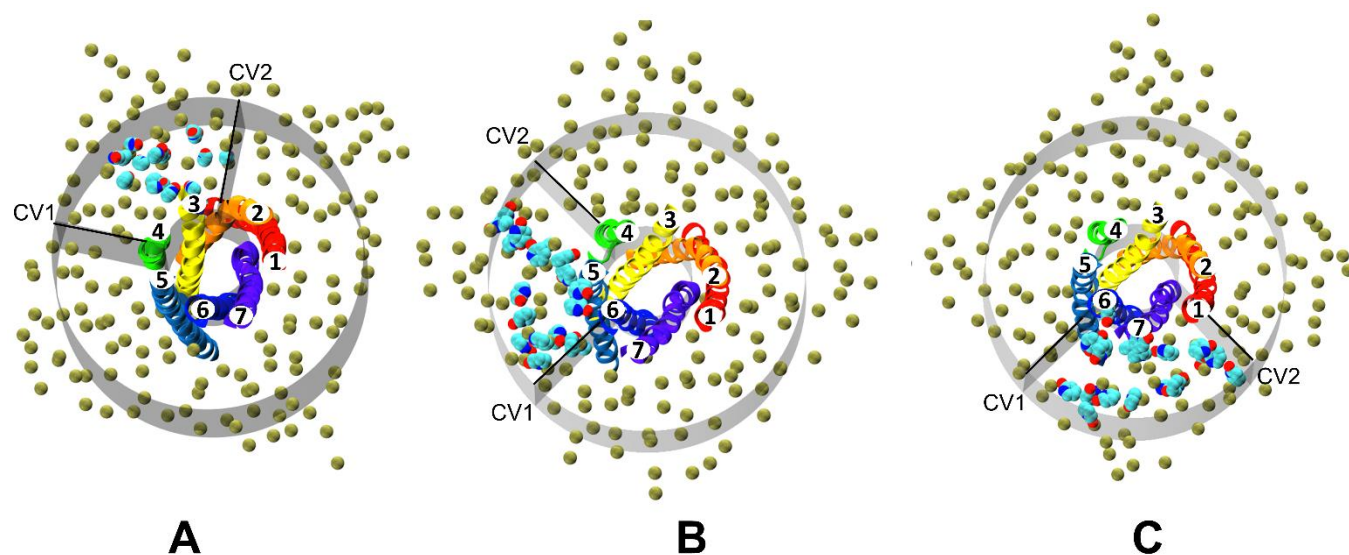
Figure S6. cAMP Accumulation assays in the absence and presence of the allosteric modulator at the D$_2$ WT, I184A and W413A mutants.
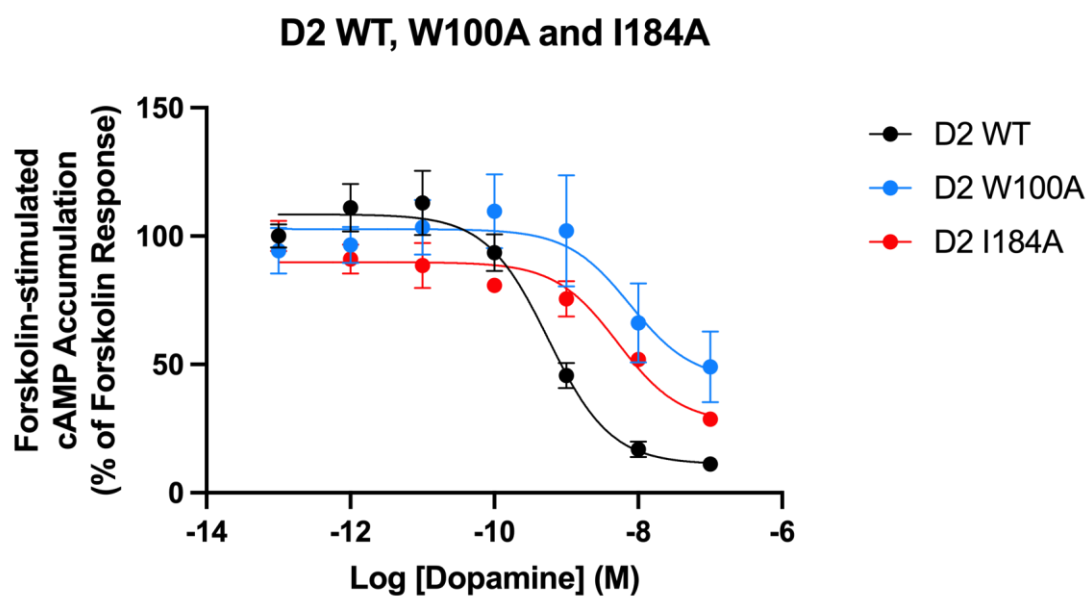
Figure S7. Expression of D$_2$ WT and mutants as measured by immunofluorescence. HEK293 cells were transiently transfected as reported in materials and methods. D2 receptor construct staining is shown in red and DAPI staining in blue.
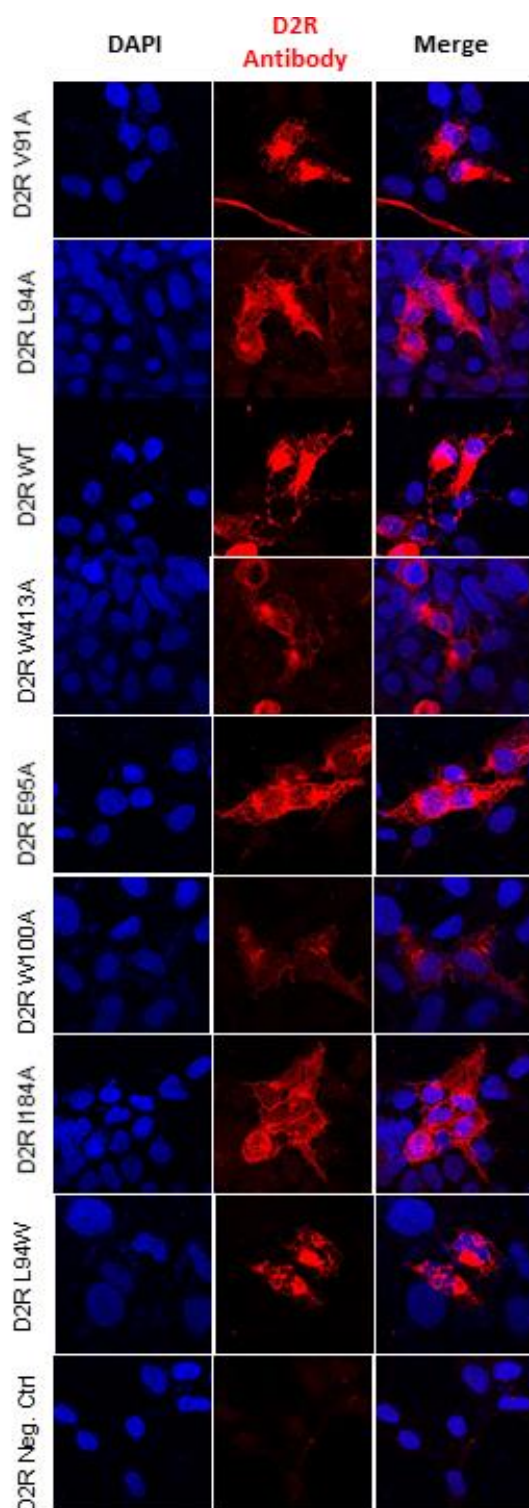
Figure S8. Cross-titration curves to calculate Kb. Concentration-response curves measuring cAMP accumulation using the endogenous agonist, dopamine, were performed with A) D2 WT, B) D2 W413A and C) D2 L94W. The UCB compound was added at 30 µM, 10 µM, 3 µM, 1 µM, 0.3 µM and 0 µM. The Allosteric EC50 shift was used to plot the curves and calculate the Kb value (D). Each data point represents the mean ± SEM of duplicate wells of five independent experiments.

	WT	W413A	L94W
Log Kb	-6.90	18.17	NA
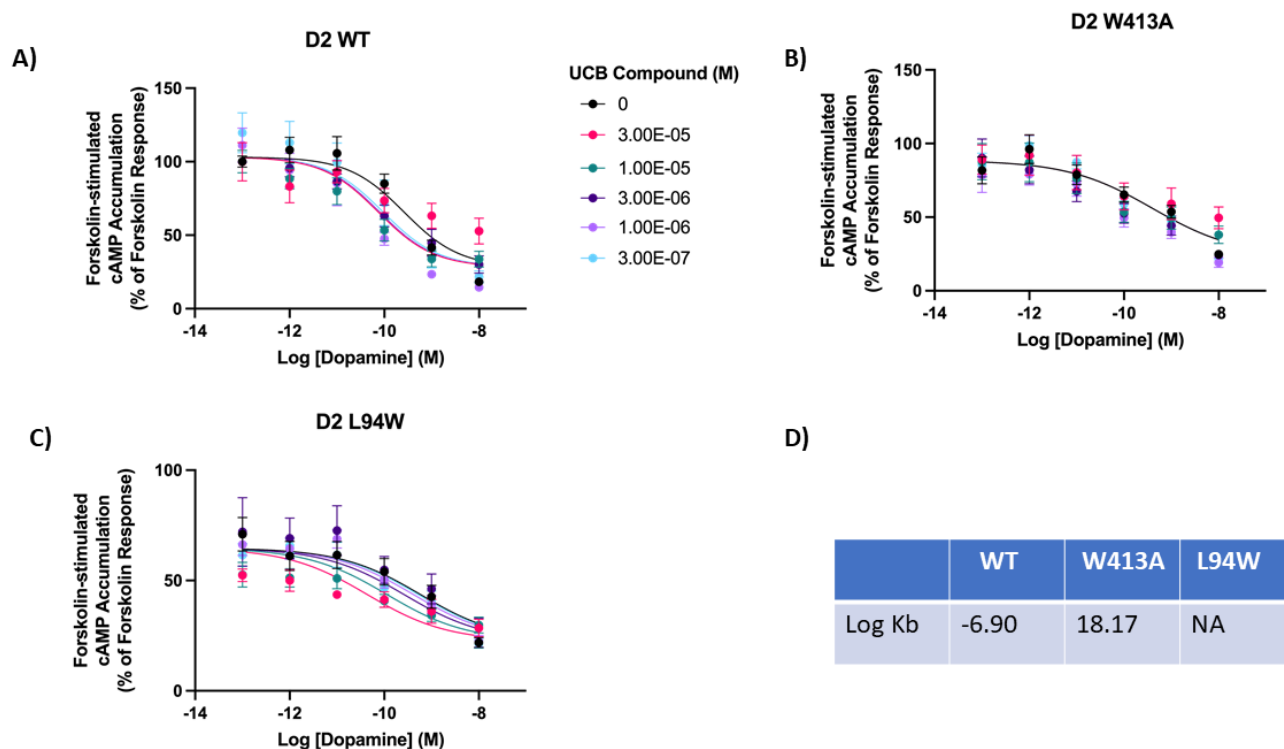
Video 1. A video of the probe confined dynamic mapping trajectory for the THP probe molecules binding to the EC side of the M$_2$ receptor. The receptor is shown in white cartoon representation with residues forming the allosteric site in stick representation. THP probe molecules are in space-filling representation and the orthosteric ligand, Iperoxo is in orange stick.

Video 2. A video of the probe confined dynamic mapping trajectory for the BTA probe molecules binding to the IC side of the β$_2$ receptor. The receptor is shown in white cartoon representation with residues forming the allosteric site in stick representation and the BTA probe molecules are in space-filling representation.

Video 3. A video of the probe confined dynamic mapping trajectory for the P2Y1 probe molecules binding to the LI of helices 1-3 of the P$_2$Y$_1$ receptor. The receptor is shown in grey cartoon representation with residues forming the allosteric site in stick representation, the P2O probe molecules are in space-filling representation and the POPC bilayer in stick representation.